

Bending and coupling losses in terahertz wire waveguides

Victoria Astley,^{1,*} Julianna Scheiman,^{1,2} Rajind Mendis,¹ and Daniel M. Mittleman¹

¹Department of Electrical and Computer Engineering, MS-366, Rice University, 6100 Main Street, Houston, Texas 77005, USA

²Present address: Hinman Box No. 4163, c/o Dartmouth College, Hanover, New Hampshire 03755, USA

*Corresponding author: vastley@rice.edu

Received October 27, 2009; revised December 22, 2009; accepted January 7, 2010;
posted January 14, 2010 (Doc. ID 119114); published February 11, 2010

We present an experimental study of several common perturbations of wire waveguides for terahertz pulses. Sommerfeld waves retain significant signal strength and bandwidth even with large gaps in the wire, exhibiting more efficient recoupling at higher frequencies. We also describe a detailed study of bending losses. For a given turn angle, we observe an optimum radius of curvature that minimizes the overall propagation loss. These results emphasize the impact of the distortion of the spatial mode on the radiative bend loss.

© 2010 Optical Society of America

OCIS codes: 260.3090, 230.7370, 240.6680.

The development of waveguides for terahertz pulses has become an active research area, as waveguides are recognized to be an enabling technology for many applications. In particular, a bare metal wire has attracted a great deal of attention, as it exhibits low loss and dispersion [1]. However, it suffers from high bending losses due to the relatively weak surface-plasmon-based guiding mechanism [2]. Despite this important drawback, the concept of transporting terahertz radiation via Sommerfeld waves on bare wires has attracted a great deal of attention [2–6], including applications in spectroscopy [7,8], subwavelength focusing [9,10], and near-field imaging [11,12]. In addition, understanding the loss mechanisms in visible and near-IR surface plasmon waveguides is very important [13], and a natural connection exists between these optical wires and their terahertz counterparts. Thus, it is important to clarify the capabilities and limitations of wire waveguides.

As a first step, we explore the efficiency with which radiation can couple from the end of one wire, across an air gap, onto the end of a second parallel wire situated on-axis with the first one. This permits us to explore the frequency-dependent diffraction that occurs in the air gap [14] and is similar to earlier work on surface plasmon coupling across a gap between two flat metal surfaces [15].

To investigate this phenomenon, we use a stainless steel wire of 1.75 mm diameter, divided into two sections of 12 cm length each. We efficiently couple terahertz radiation to the input end of the first waveguide section using a radially polarized photoconductive antenna [16]. This first section is fixed in place for the remainder of the experiment. The receiver, a fiber-coupled photoconductive antenna, is placed on opposite sides of the second waveguide section (at the output end) to establish the radial symmetry of the mode and thus ensure that the terahertz signal is coupling to the second waveguide. We then measure the terahertz radiation reaching the end of the second waveguide, while increasing the air gap between the two sections, keeping both wires aligned along a common axis.

Figure 1(a) shows the peak-to-peak amplitude of the time-domain waveforms as a function of the gap distance. Evidently, the coupling across the gap decreases with increasing gap size. However, even for rather large gaps, the spectral bandwidth is almost the same as in the case of no air gap [see inset to Fig. 1(a)]. We also observe that, with increasing gap size, the initial decrease in the signal is approximately independent of frequency, but then a clear frequency

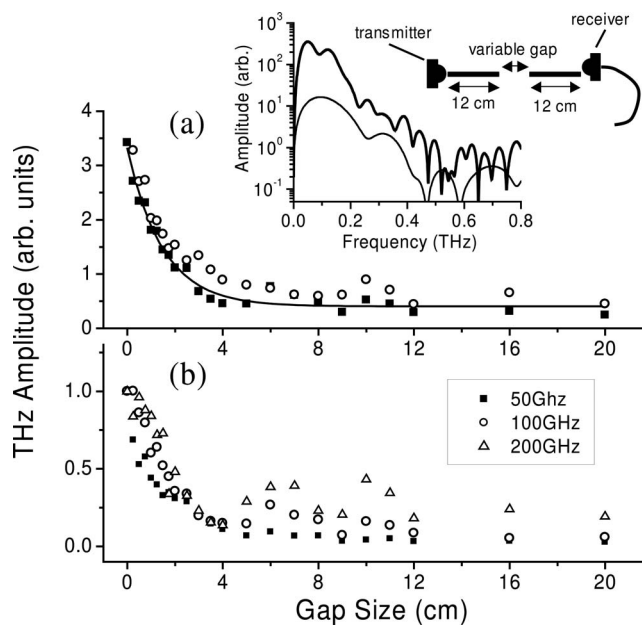


Fig. 1. (a) Peak-to-peak terahertz field amplitude for increasing gap between the two waveguide sections. Filled squares and open circles represent measurements on opposite sides of the waveguide to illustrate the symmetry of the mode at the end of the second section. The two insets show a schematic of the experiment, and the spectra for gaps of 0 (thick curve) and 12 (thin curve) cm. This illustrates that the signal decreases when a gap is inserted, but the bandwidth is essentially unchanged. (b) Relative dependence of signal strength on gap size, for a few selected spectral components. Higher frequencies diffract less strongly at the end of the first wire, and therefore couple across the gap more efficiently.

dependence emerges as higher frequencies (which diffract less strongly) recouple onto the second wire more efficiently [Fig. 1(b)].

Next, we investigate the dependence of wire-to-wire coupling on the angle between the axes of the two sections. Here, we maintain a zero end-to-end distance between the two wires, but vary the angle of the second wire axis relative to the axis of the first. The location of the receiver remains fixed relative to the second wire, as it is rotated. As seen in Fig. 2, significant signal remains even at angles as great as 30° , while angular offsets less than 10° retain the majority of the signal strength. These results imply that a small error in the angular axial alignment between waveguide sections can be tolerated.

As noted above, a disadvantage of the wire waveguide is that the Sommerfeld wave is only weakly guided, leading to high bending losses when the waveguide is curved [2,3,17]. It has been suggested that a mirror can be employed with these angled configurations of straight sections to avoid bending losses [18]. As observed above, a high angular offset between the two waveguide sections results in a greatly decreased signal. At an offset of 90° , with the two waveguide sections aligned perpendicular to one another, there is essentially zero detected signal [see Fig. 3(b)]. Next, a polished aluminum mirror of 5 cm diameter was placed at the junction of the two waveguides, at a 45° angle to both wires. As seen in Fig. 3, this has the effect of diverting (reflecting) the radiation at the output of the first waveguide onto the input of the second to allow the two sections to essentially act as a continuous wire. The terahertz signal at the end of the second wire segment is restored to almost match the reference signal, with a phase flip due to reflection and a small decrease in amplitude, most likely due at least in part to the size of the mirror. The signal strength may be further im-

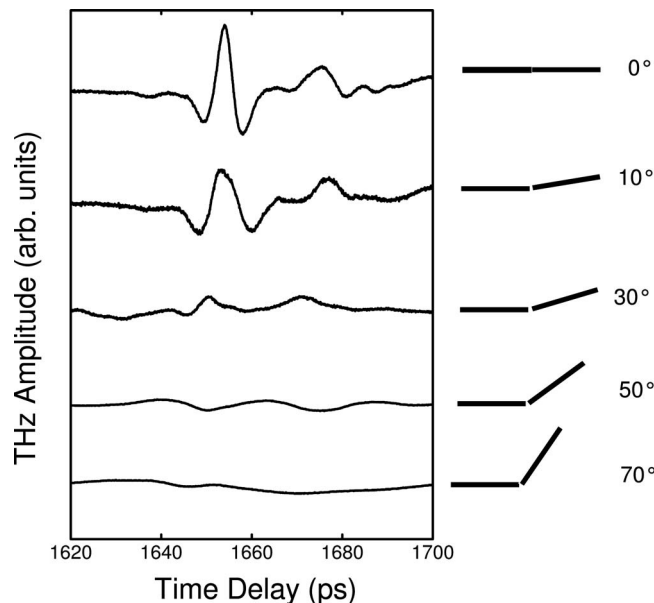


Fig. 2. Time-domain terahertz waveforms for a series of waveguide configurations at increasing angular offset, as illustrated. Significant signal remains until approximately 30° of angular displacement.

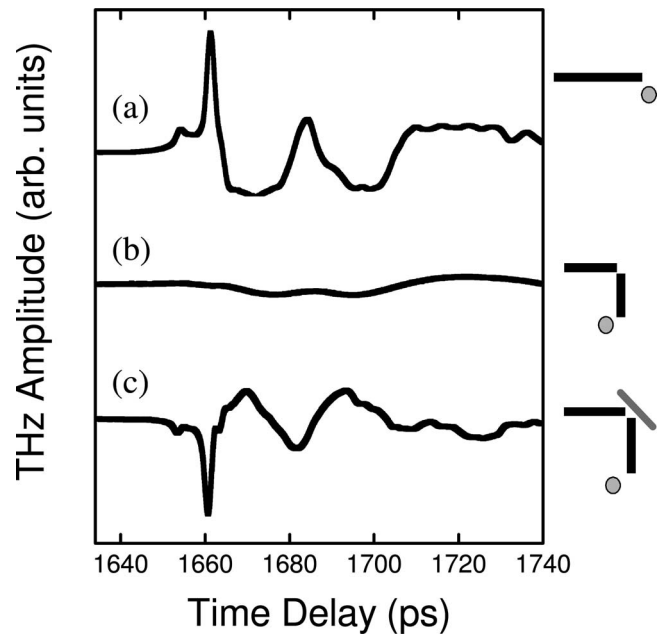


Fig. 3. Time-domain terahertz waveforms for (a) a straight waveguide, (b) two waveguide sections in a perpendicular arrangement, and (c) perpendicular waveguides with the addition of a turning mirror. The amplitude of the signal in (c) is 75% of the amplitude in (a).

proved by having the waveguide faces angled so that they are flushed with the mirror surface or by increasing the size of the mirror.

To compare this mirror geometry to that of a curved wire, we consider a circular arc with an angle of 90° and a radius of curvature R . The abrupt right-angle turn considered above (without a corner mirror) may be taken as a limiting case of this situation, with $R=0$. The total power attenuation α_T of a wave at frequency f traveling around a bend contains contributions from the radiative bend loss, which increases exponentially with decreasing radius R as $c_1 e^{-c_2 R}$ [3,19], and the ohmic loss α_{ohmic} , which is constant (independent of R) for a given arc length z . So, the amplitude transmission for an arc of angle θ is given by

$$t = e^{-(1/2)\alpha_T z} = e^{-(1/2)R\theta\alpha_T} = \exp[-R\theta(c_1 e^{-c_2 R} + \alpha_{\text{ohmic}})/2]. \quad (1)$$

For reasonable values of the parameters c_1 , c_2 , and α_{ohmic} , this is a monotonically decreasing function with increasing radius R . Here, the decreasing bend loss is compensated by the increasing ohmic loss with larger values of R (and correspondingly larger propagation distances). However, this result (inset to Fig. 4) is obviously nonphysical for very small values of R , for which the transmission should diminish rapidly [see Fig. 3(b)]. The difficulty arises from the assumption of an exponential bend loss, which is only valid for $R > \Delta$, the transverse spatial extent of the propagating mode [19]. For smaller values of R there is likely to be a little spatial overlap between the propagating modes of the straight and curved sections and therefore a reduced coupling around the curve, im-

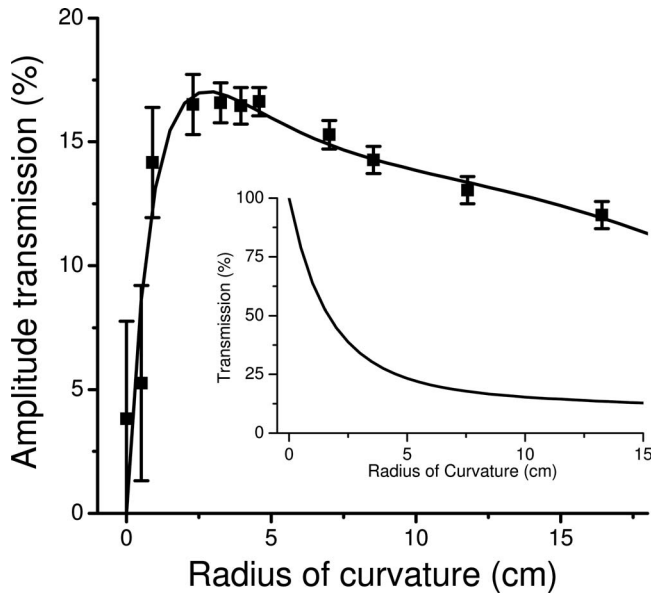


Fig. 4. Amplitude transmission after propagation along a curved waveguide section of radius R and turn angle of 90° . The transmission was determined from the time-domain waveforms by comparing the peak amplitude for the complete curved waveguide (one curved section between two straight sections) with the case of two straight sections only. The decrease at small radii results from bending loss, whereas the behavior at large radii is dictated by ohmic losses. The solid curve is a fit to the data using Eq. (2), which includes the mode size parameter Δ . Inset, an illustration of the transmission predicted by Eq. (1). This shows monotonic behavior as a function of R , which is inconsistent with the fact that the transmission must vanish as $R \rightarrow 0$.

plying a departure from this exponential form. Indeed, since the transmission must vanish for both $R \rightarrow 0$ and $R \rightarrow \infty$, it is clear that there is an optimum value for R at which the total loss for traversing a 90° bend is minimized. In order to include this effect, we modify Eq. (1) to include the spatial scale Δ which must be relevant at small R ,

$$t = \exp[-R\theta(c_1 e^{-c_2 R} + \alpha_{\text{ohmic}})/2](1 - e^{-R/\Delta}). \quad (2)$$

In our experiments, Δ is a few centimeters. This additional factor forces the transmission to zero for $R = 0$, and thus guarantees a physically reasonable result.

To confirm this behavior, we fabricate several curved waveguides of varying radii, each with a 90° turn angle. By inserting these curved waveguides between two straight waveguides and maintaining a constant receiver position relative to the end of the second straight section, we can determine the transmission for various radii of curvature for a fixed turn angle of 90° . As shown in Fig. 4, we observe a peak in the transmission at a radius of curvature $R \sim \Delta$. For smaller radii, the transmission decreases rapidly due to the bending loss, whereas for larger radii the transmission is increasingly dominated by the ohmic

loss. The maximum amplitude transmission is approximately 20%, significantly smaller than the value obtained with a corner mirror, but potentially large enough for many applications in which a mirror is not practical, such as in an endoscope [1]. The solid curve in Fig. 4 is a fit using Eq. (2). This gives $\Delta \sim 4$ cm and an ohmic loss of $\alpha_{\text{ohmic}} \sim 0.1 \text{ cm}^{-1}$. Since the data are extracted from time-domain waveforms, these values are spectrally weighted averages.

In conclusion, we have investigated the effects of gaps and bends on the propagation efficiency of terahertz wire waveguides. Our results clarify the dependence of the bending loss on the radius of curvature, emphasizing the significant role of the spatial extent of the mode and the invalidity of the conventional formalism for small radii. These results will be important in any application in which a curved wire waveguide is required and may also have bearing on the bending of surface plasmon waveguides in other regions of the spectrum [13].

This research has been supported in part by the National Science Foundation (NSF) and by the Air Force Office of Sponsored Research through the CONTACT program.

References

1. K. Wang and D. M. Mittleman, *Nature* **432**, 376 (2004).
2. T.-I. Jeon, J. Zhang, and D. Grischkowsky, *Appl. Phys. Lett.* **86**, 161904 (2005).
3. K. Wang and D. M. Mittleman, *J. Opt. Soc. Am. B* **22**, 2001 (2005).
4. M. Wachter, M. Nagel, and H. Kurz, *Opt. Express* **13**, 10815 (2005).
5. T. Akalin, A. Treizebre, and B. Bocquet, *IEEE Trans. Microwave Theory Tech.* **54**, 2762 (2006).
6. K. Wang and D. M. Mittleman, *Phys. Rev. Lett.* **96**, 157401 (2006).
7. N. C. J. van der Valk and P. C. M. Planken, *Appl. Phys. Lett.* **87**, 071106 (2005).
8. M. Walther, M. R. Freeman, and F. A. Hegmann, *Appl. Phys. Lett.* **87**, 261107 (2005).
9. H. W. Liang, S. C. Ruan, and M. Zhang, *Opt. Express* **16**, 18241 (2008).
10. V. Astley, R. Mendis, and D. M. Mittleman, *Appl. Phys. Lett.* **95**, 031104 (2009).
11. G. Shvets, S. Trendafilov, J. B. Pendry, and A. Sarychev, *Phys. Rev. Lett.* **99**, 053903 (2007).
12. M. Awad, M. Nagel, and H. Kurz, *Appl. Phys. Lett.* **94**, 051107 (2009).
13. S. Lee, S. Kim, and H. Lim, *Opt. Express* **17**, 19435 (2009).
14. J. A. Deibel, N. Berndsen, K. Wang, D. M. Mittleman, N. C. J. van der Valk, and P. C. M. Planken, *Opt. Express* **14**, 8772 (2006).
15. M. Nazarov, J.-L. Coutaz, A. Shkurinov, and F. Garet, *Opt. Commun.* **277**, 33 (2007).
16. J. A. Deibel, K. Wang, M. D. Escarra, and D. M. Mittleman, *Opt. Express* **14**, 279 (2006).
17. G. Goubau, *J. Appl. Phys.* **21**, 1119 (1950).
18. F. Sobel, F. L. Wentworth, and J. C. Wiltse, *IRE Trans. Microwave Theory Tech.* **9**, 512 (1961).
19. E. A. J. Marcatili and S. E. Miller, *Bell Syst. Tech. J.* **48**, 2161 (1969).